Inorganic Chemistry

Article

pubs.acs.org/IC

Synthesis, Characterization, and DNA Binding Properties of Ruthenium(II) Complexes Containing the Redox Active Ligand Benzo[*i*]dipyrido[3,2-*a*:2′,3′-*c*]phenazine-11,16-quinone

Simon P. Foxon, Charlotte Green, Michael G. Walker, Ashley Wragg, Harry Adams, Julia A. Weinstein, Simon C. Parker, Anthony J. H. M. Meijer,* and Jim A. Thomas*

Department of Chemistry, University of Sheffield, Sheffield, U.K. S3 7HF

Supporting Information

ABSTRACT: Synthetic methods toward ruthenium(II) complexes incorporating the benzo[*i*]dipyrido[3,2-*a*:2′,3′-*c*]phenazine-11,16-quinone ligand, qdppn, are reported. In several cases, it was found that complexes containing coordinated benzo[*i*]dipyrido[3,2-*a*:2′,3′-*c*]phenazine, dppn, could be chemically or photochemically oxidized to their qdppn analogues. Since this method was not possible in all the cases, a new, higher yielding, convenient synthesis of qdppn was developed. The crystal structure of the complex $[Ru(phen)_2(qppn)](PF_6)_2$ (phen = 1,10-phenanthroline) which was synthesized from free qdppn reveals that a combination of $\pi-\pi$ stacking between coordinated phen and qdppn units, as well as anion-ligand hydrogen bonding, define large hexagonal channels which are occupied by anions and solvent molecules. Electrochemical and photophysical studies reveal that the new qdppn-based complexes are not luminescent and, in contrast to their dppn analogues, they are also poor singlet oxygen sensitizers. Time-resolved studies and density functional theory (DFT) calculations indicate that optical properties of the new complexes are due to a short-lived charge separated state involving the quinone moiety of qdppn. The DNA binding properties of the new complexes have also been investigated. It was found that they are intercalators, displaying binding affinities which are comparable to their dppn analogues.

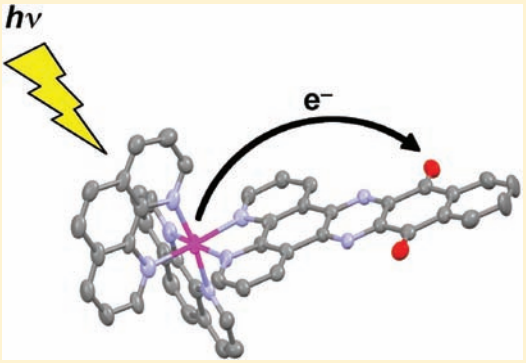

INTRODUCTION

Polypyridyl d^6 transition metal complexes based on metal centers such as Ru^{II}, Os^{II}, Re^{I}, and Ir^{III} possess attractive photophysical properties: they typically absorb light in the visible wavelength region, possess long-lived metal-to-ligand charge transfer (^{3}MLCT) excited states, are luminescent, and have rich redox chemistry.[1] Such complexes have been widely used for a variety of functions including chromophores for energy conversion[2] and molecular devices.[3] In this context, ligands containing quinone moieties are of particular interest as components in chromophore quencher systems, as they possess good acceptor properties and can function as reversible $2e^-$ redox couples.[4,5]

In this context, the Loeb and Meyer groups reported on a Re^{I} chromophore quencher system containing 12,17-dihydronaphtho[2,3-*h*]dipyrido[3,2-*a*:2′,3′-*c*]-phenazine-12,17-dione, aqphen, as the acceptor ligand, Figure 1.[6] They found that in the excited state, an electron is largely localized on the quinone portion of aqphen. Around the same time, Maiya and colleagues investigated the redox and DNA binding properties of $[Ru(phen)_2(aqphen)]^{2+}$ (phen = 1,10-phenanthroline).[7,8]

More recently, the Liu and Hauser groups have employed aqphen as an acceptor moiety in the construction of Ru^{II}-based chromophore quencher systems that display long-lived charge separated states.[9] In related work, the Loeb group has also described the five step synthesis of an analogue of aqphen, benzo[*i*]dipyrido[3,2-*a*:2′,3′-*c*]phenazine-11,16-quinone (qdppn) and briefly outlined the syntheses and absorption spectra of two $[Re(L)CO)_3(qdppn)]$ complexes (L = Cl, CF_3SO_3).[10] In a later study, Rao et al. revealed that photoirradiation of the complex $[Ru(dtb\text{-}bpy)_2(dppn)]^{2+}$ (dtb-bpy = 4,4-di-*tert*-butyl-2,2-bipyridine; dppn = benzo[*i*]-dipyrido[3,2-*a*:2′,3′-*c*]phenazine) in aerobic conditions produced $[Ru(dtb\text{-}bpy)_2(qdppn)]^{2+}$ in essentially quantitative yields.[11] However, this brief report did not describe any photophysical studies on this system. Metal complexes containing ligands related to aqphen and qdppn have also been investigated as DNA binding substrates.

The DNA light-switch complex,[12] $[Ru(LL)_2(dppz)]^{2+}$ (LL = 2,2′-bipyridine, 1,10-phenanthroline) has attracted particular attention (dppz = dipyrido[3,2-*a*:2′,3′-*c*]phenazine). Its luminescence properties offer a simple means of monitoring DNA binding: emission from aqueous solutions of the complex is quenched by water molecules, while binding to DNA through intercalation enhances luminescence by several orders of magnitude.[13,14] With the aim of identifying novel mono- and oligonuclear DNA binding substrates, we have investigated the

Received: September 1, 2011
Published: December 6, 2011

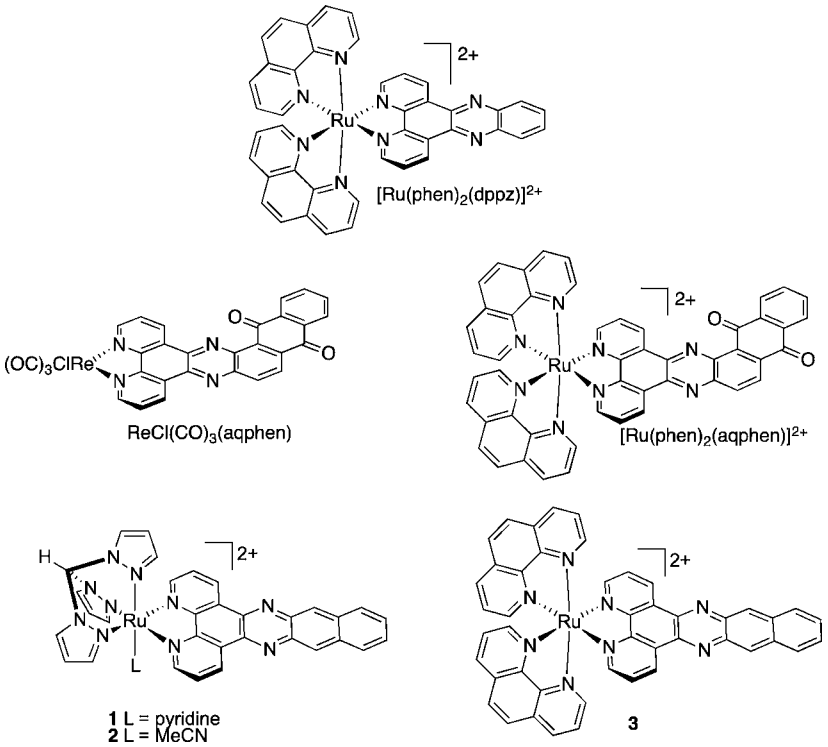

Figure 1. Structure of $[Ru(phen)_2(dppz)]^{2+}$ (top) and previously reported aqphen (middle row) and dppn (bottom row) complexes relevant to this study.

DNA binding properties of achiral [Ru(tpm)dppz]-based systems.[15] More recently we have extended these studies to report on the properties of new $[Ru^{II}(tpm)(L)(dppn)]$ complexes **1** and **2** (dppn = benzo[*i*]dipyrido[3,2-*a*:2′,3′-*c*]phenazine, tpm = tris(1-pyrazolyl)methane, L = Cl^-, pyridine (py), and acetonitrile (MeCN)), Figure 1.[16,17] This was partly motivated by the fact that, although complexes containing dppz have been much reported and studied, until recently there were much fewer reports on Ru(dppn) based systems.[18,19]

It was found that, while the overall binding affinity of the dppn complexes were similar to those of their dppz analogues,[16] their photophysical properties are very different: **1** and **2** (as well as $[Ru(phen)_2(dppn)]^{2+}$, **3**) are virtually nonemissive in all solvents and do not show DNA-induced luminescence changes. Instead photoexcitation of these Ru(dppn) systems leads to a dppn-based $\pi\rightarrow\pi^*$excited state that is a highly efficient singlet oxygen sensitizer[17] capable of efficiently cleaving DNA.[20] Presumably the clean conversion of ruthenium(II) coordinated dppn into qdppn observed by Rau et al. occurs through the reaction with singlet oxygen that is generated from the dppn-based $\pi\rightarrow\pi^*$excited state.

Herein we report on the photophysical, electrochemical, and DNA binding properties of three new Ru^{II}(qdppn) systems and also a high yielding convenient route to the free ligand itself.

EXPERIMENTAL SECTION

Materials. Solvents were dried and purified using standard literature methods, while other commercially available materials were used as received. 1,10-Phenanthroline-5,6-dione[21] and the complexes $[Ru(phen)_2Cl_2]$,[22] $[(tpm)Ru(dppn)(py)][PF_6]_2$ (**1**), $[(tpm)Ru(dppn)(MeCN)][PF_6]_2$ (**2**), and $[Ru(phen)_2(dppn)]^{2+}$ (**3**) were synthesized using previously reported methods.[16,18] The buffer used for UV−visible titrations consisted of 25 mM NaCl and 5 mM tris (pH 7.0) made with doubly distilled water (Millipore). Calf thymus DNA (CT-DNA) was purchased from Sigma and was purified until $A_{260}/A_{280} > 1.9$. Concentrations of CT-DNA solutions were determined spectroscopically using the extinction coefficient of CT-DNA (ε = 6600 $dm^3\ mol^{-1}\ cm^{-1}$ at 260 nm).

Instrumentation. Standard ^1H NMR spectra were recorded on either a Bruker AM250 or AMX400 spectrometer. FAB mass spectra were obtained on a Kratos MS80 machine working in positive ion mode, with *m*-nitrobenzyl alcohol matrix. UV−visible spectra were recorded on a Unicam UV2 spectrometer or Cary 50 spectrometer in twin beam mode. Spectra were recorded in matched quartz cells and were baseline corrected. Steady-state luminescence emission spectra were recorded either in aerated acetonitrile or tris buffer solutions on a Hitachi F-4500 instrument. Cyclic voltammograms were recorded using an EG&G model Versastat II potentiostat and the EG&G electrochemistry power suite software package. Potentials were measured against a Ag/AgCl reference electrode, and ferrocene was used as an internal reference.

Nanosecond Flash Photolysis studies were conducted on the home-built setup. The tripled output of Q-switched Nd:YAG laser LS-2137U (LOTIS TII) was used as the excitation source (7 ns, 355 nm), while the probing was performed with a steady-state 150 W Hamamatsu Arc Xe lamp. The probe beam was detected by a monochromator equipped with a home-built detector unit, based on FEU-118 PMT. Detector current output was coupled into Tektronix TDS 3032B digital oscilloscope and subsequently transferred to the computer. The instrumental response function is estimated as about 22 ns fwhm. Sample solutions in MeCN were degassed by the freeze−pump−thaw technique in 10 mm quartz cells and subsequently saturated with argon. Sample solutions in water were deoxygenated with the freeze−pump−thaw technique (with careful freezing of the sample) in 10 mm quartz cells, and subsequently filled with argon. The excitation energies and sample concentrations used were 2.5−5 mJ and 20−35 μM respectively. Singlet oxygen yields were determined through a previously described method.[17]

DNA Titration Protocol. The DNA titration protocol has been previously reported.[15]

Syntheses. 2,3-Diamino-1,4-naphthoquinone was readily synthesized in good yields using the method described by Winkelmann.[23] Although dppn has been reported before, a synthetic procedure or full

dx.doi.org/10.1021/ic201914h | *Inorg. Chem.* 2012, 51, 463−471

assignment of its ^{1}H NMR spectrum has never been reported. Previous reports have briefly mentioned that it was synthesized using an adaptation of the method used for dppz, that is, by condensation of 1,10-phenanthroline-5,6-dione (**dpq**) and 2,3-diaminonaphthalene in ethanol. In our hands, although these conditions produced a relatively good yield of crude dppn, it was obtained as a gelatinous precipitate that was problematic to isolate and purify. What follows is a facile procedure that consistently gave high yields.

Benzo[i]dipyrido[3,2-a:2′,3′-c]phenazine (dppn). 1,10-Phenanthroline-5,6-dione (1.00 g, 4.76 mmol) and 2,3-diaminonaphthalene (0.84 g, 5.31 mmol) in methanol (150 cm^3) were heated under reflux for 1 h, during which time a bright-orange colored precipitate formed. The precipitate was collected, washed subsequently with water (50 cm^3), methanol (50 cm^3) and diethyl ether (50 cm^3), and dried in vacuo to afford dppn (1.50 g, 94%) as an orange colored solid. Elemental Analysis: Found: C, 73.5; H, 4.0; N, 15.8, ($C_{22}H_{12}N_4$·1.5H_2O requires C, 73.5; H, 4.2; N, 15.6%); ^{1}H NMR: δ_H(250 MHz; $CDCl_3$) 7.60 (2H, [H_b, H_b′], dd, J_{fe}′ = 4.4 Hz, J_{fe} = 8.0 Hz), 7.76 (2H, [H_f, H_f′], dd, J_{ba} = 3.4 Hz, J_{bc} = 6.7 Hz), 8.16 (2H, [H_e, H_e′], dd, J_{ef}′ = 3.4 Hz, J_{ef} = 6.7), 8.87 (2H, [H_d, H_d′], s), 9.22 (2H, [H_a, H_a′], d, J_{ab} = 4.4 Hz) and 9.56 (2H, [H_c, H_c′], d, J_{cb} = 8.0 Hz); ^{13}C NMR: δ_C(126 MHz; $CDCl_3$) 152.7(CH), 148.8, 142.1, 138.7, 134.4, 133.9(CH), 128.6(CH), 128.0, 127.8(CH), 127.1(CH) and 124.3(CH); *m*/*z* (TOF MS-ES) 333 (MH^+). IR/cm^{-1}: 1629(w), 1584(w), 1564(w), 1515(w), 1472(w), 1409(m), 1539(m), 1274(w), 1070(m), 1033(w), 892(w), 872(s), 817(m), 740(s).

*[Ru(tpm)(qdppn)(py)](PF$_6$)$_2$ [**4**](PF$_6$)$_2$.* [Ru(tpm)(dppn)(py)][(PF_6)$_2$] (0.12 g, 0.11 mmol) and $(NH_4)_2S_2O_8$ (0.20 g) were refluxed for 3 h in acetonitrile/water (3:1) (75 cm^3). The dark red colored solution was allowed to cool. Saturated aqueous NH_4PF_6 (∼2 cm^3) was added, and the solution was concentrated in vacuo to induce precipitation. The precipitate was collected by filtration and washed with water (3 × 10 cm^3) and diethyl ether (10 cm^3) to yield **4** as a red colored solid (0.08 g, 73%). Elemental Analysis: Found: C, 41.79; H, 2.22; N, 14.21. $C_{37}H_{25}F_{12}N_{11}O_2P_2Ru$·$H_2O$ requires C, 41.74; H, 2.56; N, 14.47%; ^{1}H NMR: δ_H(250 MHz; CD_3CN) 6.17 (1 H, t, tpm−*H*), 6.40 (1 H, d, tpm−*H*), 6.81 (2 H, t, tpm−*H*), 7.03 (2 H, m, py−*H*), 7.38 (2 H, m, py−*H*), 7.70 (1 H, m, py−*H*), 8.05−8.11 (6 H, m, 2tpm−*H*, 4Ar−*H*), 8.36 (1 H, d, tpm−*H*), 8.50 (2 H, dd, Ar−*H*), 8.60 (2 H, d, tpm−*H*), 9.12 (1 H, s, tpm−*H*), 9.17 (2 H, d, Ar−*H*), 9.78 (2 H, d, Ar−*H*); ^{13}C NMR (CD_3CN, 500 MHz) *δ*: 181.8 (quinone), 157.5, 154.1, 152.5, 148.7, 146.2, 145.2, 143.9, 138.5, 136.9, 136.7, 136.6, 135.5, 135.4, 134.9, 131.5, 128.6, 127.8, 236.4, 222.0, 209.5, 77.2 [$(pz)_3CH$]; TOF MS-ES: *m*/*z* = 902 (M − PF_6, 65%), 756 (M − 2PF_6, 85%), 678 (M − 2PF_6, −C_5H_5N, 10%); IR/cm^{-1}: 1684(w) [C═O], 1590(w), 1531(w), 1489(w), 1444(w), 1407(m), 1378(w), 1342(w), 1310(w), 1285(m), 1239(m), 1220(m), 1171(w), 1130(w), 1096(m), 1056(w), 986(w), 832(s), 781(w), 763(w), 703(w).

*[Ru(tpm)(qdppn)(MeCN)](PF$_6$)$_2$ [**5**](PF$_6$)$_2$.* [Ru(tpm)(dppn)(MeCN)][(PF_6)$_2$] (0.11 g, 0.11 mmol) and $(NH_4)_2S_2O_8$ (0.20 g) were refluxed for 3 h in acetonitrile/water (3:1) (75 cm^3) as described above to yield **5** as a red solid (0.091 g, 80%). Elemental analysis: found: C, 39.82; H, 2.12; N, 14.54. ($C_{34}H_{23}F_{12}N_{11}O_2P_2Ru$·$H_2O$ requires C, 39.78; H, 2.45; N, 15.01%); ^{1}H NMR: δ_H(250 MHz; CD_3CN) 2.04 (3 H, s, [Ru]−CH_3CN), 6.24 (1 H, t, tpm−*H*), 6.60 (1 H, d, *J* 2.1, tpm−*H*), 6.81 (2 H, t, tpm−*H*), 8.06 (2 H, dd, Ar−*H*), 8.15 (2 H, dd, Ar−*H*), 8.36 (1 H, d, tpm−*H*), 8.46 (2 H, dd, Ar−*H*), 8.49−8.52 (4 H, m, tpm−*H*), 9.05 (1 H, s, tpm−*H*), 9.20 (2 H, dd, Ar−*H*), 9.76 (2 H, dd, Ar−*H*); ^{13}C NMR (CD_3CN, 500 MHz) *δ*: 181.8 (quinone), 157.4, 152.9, 148.9, 146.3, 146.0, 143.5, 136.6, 135.6, 134.9, 130.5, 128.7, 127.8, 126.9, 110.6, 77.2 [$(pz)_3CH$] 4.3 [RuNCCH$_3$]; TOF MS-ES: *m*/*z* = 864 (M − PF_6, 30%), 718 (M − 2PF_6, 30%), 677 (M − 2PF_6, −CH_3CN, 100%). IR/cm^{-1}: 3640(w), 3136(w), 1689(w) [C═O], 1629(w), 1591(w), 1531(w), 1481(w), 1442(w), 1408(m), 1372(w), 1342(m), 1310(m), 1283(m), 1239(m), 1222(m), 1177(w), 1129(w), 1095(m), 1058(w), 968(m), 827(s), 760(w), 730(s).

Benzo[i]dipyrido[3,2-a:2′,3′-c]phenazine-11,16-quinone (qdppn). 1,10-Phenanthroline-5,6-dione (dpq) (600 mg, 2.85 mmol) and 2,3-diamino-1,4-naphthoquinone (537 mg, 2.85 mmol) were suspended in glacial acetic acid (50 cm^3) and the purple solution heated at reflux for 3 h during which time the color changed to brown. The brown reaction mixture was allowed to cool to room temperature, and the yellow-green precipitate was collected by filtration, washed with ethanol, diethyl ether, and dried. Yellow-green solid: 800 mg, 78%. Anal. Calcd (%) for $C_{22}H_{10}N_4O_2$·1/4H_2O: C, 72.03; H, 2.88; N, 15.27. Found: C, 71.94; H, 2.68; N, 15.35. ^{1}H NMR (400 MHz, $CDCl_3$) *δ*/ppm: 9.81 (2H, dd, J_{HH} = 1.7, 8.2 Hz), 9.41 (2H, dd, J_{HH} = 1.7, 4.4 Hz), 8.54 (2H, dd, J_{HH} = 3.4, 5.9 Hz), 7.98 (2H, dd, J_{HH} = 3.4, 5.8 Hz), 7.93 (2H, dd, J_{HH} = 4.4, 8.1 Hz). ^{13}C NMR ($CDCl_3$) *δ*/ppm: 181.0 (C═O), 154.0, 148.4, 144.0, 143.6, 135.4, 133.6, 128.2, 126.6, 124.8. EIMS *m*/*z* = 362 [M^+]. IR/cm^{-1}: 1681(m) [*ν*C═O], 1586(m), 1575(m), 1526(m), 1513(m), 1463(m), 1452(m), 1370(m), 1338(m), 1324(m), 1311(m), 1267(m), 1233(m), 1218(s), 1122(m), 1079(m), 1046(m), 1032(m), 959(m), 809(s), 740(s), 720(s).

*[Ru^{II}(phen)$_2$(qdppn)][PF$_6$]$_2$ [**6**](PF$_6$)$_2$.* Benzo[*i*]dipyrido[3,2-*a*:2′,3′-*c*]phenazine-11,16-quinone (qdppn) (104 mg, 0.29 mmol) and [$Ru(phen)_2Cl_2$]·2H_2O (136 mg, 0.22 mmol) were suspended in anhydrous ethylene glycol (30 cm^3) and heated at reflux for 3 h under nitrogen. The dark orange solution was allowed to cool to room temperature. An aqueous solution of NH_4PF_6 (∼10 cm^3) was added to the orange solution, followed by water (∼100 cm^3), and the resulting orange precipitate was collected by filtration, washed with copious amounts of water, and dried in vacuo. The crude material was purified by anion metathesis via the chloride salt using tetrabutylammonium chloride in acetone. The chloride complex was then converted back to the hexafluorophosphate salt using aqueous NH_4PF_6. Dark orange solid: 294 mg, 78%. ^{1}H NMR (400 MHz, CD_3CN) *δ*/ppm: 9.64 (2H, dd, J_{HH} = 1.2, 8.3 Hz), 8.64 (2H, dd, J_{HH} = 1.2, 2.9 Hz), 8.61 (2H, dd, J_{HH} = 1.2, 3.2 Hz), 8.47 (2H, dd, J_{HH} = 3.2, 5.7 Hz), 8.27 (4H, s), 8.22 (2H, dd, J_{HH} = 1.2, 5.4 Hz), 8.19 (2H, dd, J_{HH} = 1.2, 5.4 Hz), 8.05 (2H, dd, J_{HH} = 3.2, 5.7 Hz), 8.03 (2H, dd, J_{HH} = 1.2, 5.1 Hz), 7.84 (2H, dd, J_{HH} = 5.4, 8.3 Hz), 7.68−7.62 (4H, m). Anal. Calcd (%) for $C_{46}H_{26}F_{12}N_8O_2P_2Ru$·$H_2O$: C, 48.82; H, 2.49; N, 9.90. Found: C, 48.68; H, 2.36; N, 9.80. TOF-MSES: *m*/*z* = 969 [M − PF_6^-]$^+$, 412 [M − 2PF_6^-]$^{2+}$. IR/cm^{-1}: 1684(s) [*ν*C═O], 1587(m), 1526(m), 1451(m), 1430(m), 1408(m), 1395(m), 1372(m), 1338(m), 1324(m), 1308(m), 1267(m), 1222(m), 1176(m), 1126(m), 1079(m), 1032(m), 967(m), 825(s), 810(s), 731(m), 719(s).

DFT Calculations. Calculations were performed on compounds **4**−**6** using the Gaussian 2009 program package.[24] Gaussian was compiled using the Portland compiler v 8.0−2 on an EMT64 architecture using Gaussian-supplied versions on BLAS and ATLAS. In all calculations we used the B3LYP functional.[25] The basis set used was the Stuttgart-Dresden pseudopotential[26] on Ru^{II} and 6-311G** on all other elements.[27] We modeled the effect of solvent in all calculations using the PCM method as implemented in Gaussian[28] using the standard parameters for acetonitrile. In all our calculations ultrafine integrals were used. The largest calculation was performed for **6** with 1200 basis functions and 390 electrons.

The following procedure was adopted for all calculations. First we optimized the structure of the relevant compound to obtain the ground state energy and structure. We also obtained frequencies to verify a true minimum. From the converged minimum energy structure we obtained the excited states using the time-dependent DFT (TD-DFT) formalism,[29] whereby 100 states were obtained in each calculation. Some analysis was done using the Gausssum program.[30] The Lorentzian width on the spectra is 3000 cm^{-1} for each individual transition.

X-ray Crystallography. X-ray crystallographic data for [**6**](PF_6)$_2$ are summarized in Table 1. A single crystal was coated with hydrocarbon oil and attached to the tip of a glass fiber and transferred to a Bruker SMART diffractometer with an Oxford Cryosystems low-temperature system. Data were collected using graphite-monochromated Mo−K*α* radiation (*λ* = 0.71073 Å). The data were corrected for Lorentz and polarization effects. The structure solution and refinement was carried out using SHELXS-97 and SHELXL-97 respectively.[31,32] The structure was solved by Patterson methods and refined by full-matrix least-squares methods on F^2. Hydrogen atoms were placed

dx.doi.org/10.1021/ic201914h | Inorg. Chem. 2012, 51, 463−471

Table 1. Crystallographic Data for $[6](PF_6)_2$

empirical formula	$C_{46}H_{26}F_{12}N_8O_2P_2Ru$
M	1113.76
crystal system	rhombohedral
space group	$R\bar{3}c$
crystal dimensions/mm	0.11 × 0.09 × 0.04
a/ Å	36.596(5)
b/ Å	36.596(5)
c/ Å	19.741(3)
α/ deg	90
β/ deg	90
γ/ deg	120
U/ Å^3	22897(6)
Z	18
D_c/Mg m^{-3}	1.454
F(000)	10008
M(Mo−Kα)/ mm^{-1}	0.460
final $R1$ (on F)	0.1013
Final $wR2$ (on F)	0.2977

geometrically and refined with a riding model and the U_{iso} constrained to be 1.2 (1.5 for methyl groups) times U_{eq} of the carrier atom. All non-hydrogen atoms were refined anisotropically.

RESULTS AND DISCUSSION

Synthetic Studies. As reported by Rao et al.,[11] it was discovered that pure acetonitrile solutions of hexafluorophosphate salt of **1** and **2** exposed to light and air slowly converted to a new product. NMR and MS spectroscopic studies confirmed that the new products were the qdppn analogues **4** and **5** (Figure 2).

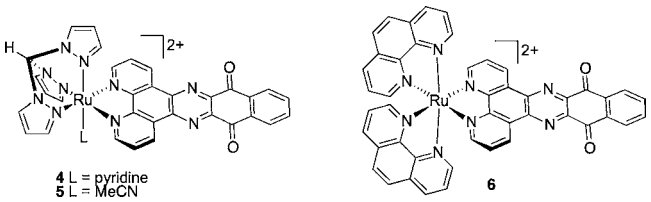

Figure 2. New Ru(qdppn) complexes synthesized and studied in this report.

Prompted by this discovery, we investigated methods to synthesize isolated samples of **1** and **2** more quickly and efficiently. The MacDonnell and Campagna groups have previously reported that, when coordinated to $[Ru^{II}(phen)_2]$ units, the ligand 9,11,20,22-tetraazatetrapyrido[3,2-*a*:2′3′-*c*:3″,2″-*l*:2‴,3‴-*n*]pentacene (tatpp) is stable on exposure to light,[33] but is oxidized by persulfate to produce coordinated 9,11,20,22-tetraazatetrapyrido[3,2-*a*:2′3′-*c*:3″,2″-*l*:2‴,3‴-*n*]-pentacene-10,21-quinone (tatpq) in good yield.[27] Given the structural similarities between dppn and tatpp we investigated the reaction of **1** and **2** with $(NH_4)_2(S_2O_8)$.

We found that by treating refluxing aqueous acetonitrile solutions of **1** or **2** with ammonium persulfate complexes **4** and **5** were produced in good yields. Following precipitation as hexafluorophosphate salts, the new complexes were found to be analytically pure by ^{1}H and NMR, IR, UV−Vis, and mass spectroscopies without the need of further workup. Interestingly, in our hands, attempts to oxidize complex **3** through the same route were less successful, with intractable mixtures of **3** and its oxidation product, **6**, being produced.

In an effort to cleanly synthesize complex **6** the synthesis of free qdppn was further explored. Since Rao et al. have shown that uncoordinated dppn is not efficiently photoconverted to qdppn[11] and the ammonium persulfate oxidation of coordinated dppn in **1** and **2** was so clean, we decided to explore the possibility of preparing free qdppn directly from dppn using conditions very similar to those employed for the oxidation of **1** and **2**, followed by the addition of excess water. However, while we found that it was possible to isolate qdppn from the reaction mixture, because of the poor solubility of dppn this method was not consistently reproducible, and thus not amenable to a large scale-up. Therefore, we chose to synthesize the ligand from 2,3-diamino-1,4-naphthoquinone. Although this intermediate is not commercially available, it is readily synthesized from commercial materials; thus, this new route produces qdppn in fewer steps and in higher yields using readily available starting materials. Using free qdppn synthesized by this method, we went on to synthesize a pure sample of $[Ru(phen)_2(qdppn)]^{2+}$ (**6**), which, as far as we are aware, has not been previously reported.

Spectroscopic Studies. Analysis of the ^{1}H NMR spectra of the new complexes was facilitated by a comparison of the spectra of free dppn and qdppn. In $CDCl_3$, because of quinone formation, the singlet resonance at δ = 8.87 ppm observed in the spectrum of dppn is absent in the spectrum of qdppn. The other five resonances in qdppn are significantly shifted downfield relative to the corresponding dppn resonances, with the protons residing on the "phenazine" moiety of dppn undergoing the largest change in chemical shifts. This reflects the change in electronic structure upon oxidation, the close proximity of the electron-withdrawing quinone moieties causing these protons to become deshielded. The carbonyl carbons of the quinone moiety in qdppn, which are absent in dppn, appear at 181.0 ppm in the ^{13}C NMR spectrum.

As illustrated by comparison of the ^{1}H NMR spectra of **2** and **5** in MeCN, Figure 3, the qdppz-based complexes demonstrate

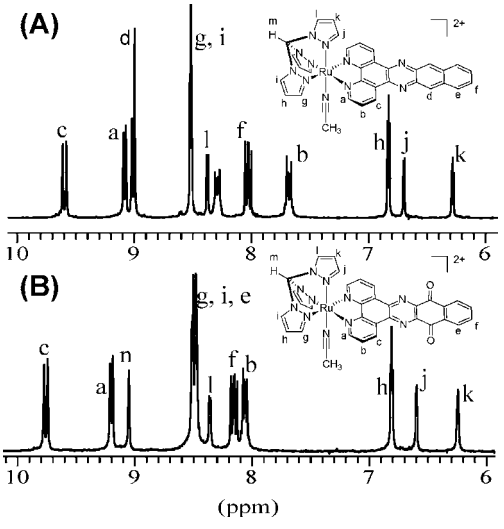

Figure 3. ^{1}H NMR (250 MHz; CD_3CN) spectral changes upon oxidation of (A) **2** to (B) **5**.

similar spectral changes because of the oxidation of the aromatic ring of the dppn ligand. As for the free ligands, the key spectral difference due to quinone formation is the disappearance in **5** of the singlet resonance observed at δ = 9.04 ppm in **2**

dx.doi.org/10.1021/ic201914h | *Inorg. Chem.* 2012, 51, 463−471

Table 2. Selected Bond Lengths (Å) and Angles (deg) for $[6](PF_6)_2$

Selected Bond Lengths (Å)			
Ru(1)−N(1)	2.062(7)	Ru(1)−N(2)#1	2.048(7)
Ru(1)−N(1)#1	2.062(7)	Ru(1)−N(3)	2.044(6)
Ru(1)−N(2)	2.048(7)	Ru(1)−N(3)#1	2.044(6)
Selected Bond Angles (deg)			
N(1)−Ru(1)−N(1)#1	94.4(3)	N(1)#1−Ru(1)−N(3)#1	93.1(2)
N(1)−Ru(1)−N(2)	79.4(3)	N(2)−Ru(1)−N(2)#1	171.7(3)
N(1)−Ru(1)−N(2)#1	94.9(3)	N(2)−Ru(1)−N(3)	92.5(2)
N(1)−Ru(1)−N(3)	93.1(2)	N(2)−Ru(1)−N(3)#1	93.8(3)
N(1)−Ru(1)−N(3)#1	170.3(2)	N(2)#1−Ru(1)−N(3)	93.8(3)
N(1)#1−Ru(1)−N(2)	94.9(3)	N(2)#1−Ru(1)−N(3)#1	92.5(2)
N(1)#1−Ru(1)−N(2)#1	79.4(3)	N(3)−Ru(1)−N(3)#1	80.2(3)
N(1)#1−Ru(1)−N(3)	170.3(2)		

and similar downfield shifts of the relevant protons. In the ^{13}C NMR spectrum of **4**, **5**, and **6** the carbonyl carbons of the qdppn quinone moiety, appear at almost at the same position as those in the free qdppn. The IR spectra of the complexes all display a carbonyl stretch at a frequency within 10 cm^{-1} of that the free qdppn ligand, which is observed at 1686 cm^{-1}.

X-ray Crystallography. X-ray quality crystals of complex $[6](PF_6)_2$ were grown through vapor diffusion of diethyl ether into acetonitrile solutions of the hexafluorophosphate salt. A summary of bond lengths and bond angles for the complex can be found in Table 2.

The coordination geometry around the ruthenium(II) center Ru(1) is close to octahedral, with little variation in Ru−N bonds lengths (2.044(6)−2.062(7) Å), Figure 4a. However, the

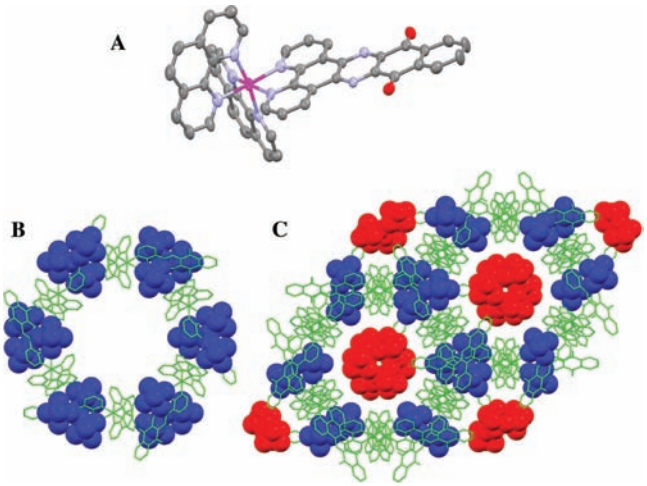

Figure 4. (A) Ellipsoid diagram of the cation from the $[6](PF_6)_2$ structure. (B) Hexagonal channels composed of cations and one set of symmetry related hexafluorophosphate anions (shown in blue). The channels are defined by $\pi-\pi$ stacking between coordinated phen and qdppn units, as well as anion-ligand hydrogen bonding. (C) A view down the C-axis of the unit cell of the structure showing how the channels are occupied by a second set of symmetry related hexafluorophosphate anions (shown in red).

unit cell reveals an array of noncovalent interactions resulting in a complex extended structure. A combination of $\pi-\pi$ stacking between coordinated phen and qdppn units, as well as anion-ligand hydrogen bonding, define hexagonal channels around 13.5−14 Å in diameter (Figure 4b), filled by further hexafluorophosphate anions (Figure 4c).

Electrochemical Studies. The electrochemical properties of the new qdppn-based complexes were investigated by cyclic voltammetry, see Table 3. All the complexes display a single

Table 3. Electrochemical Data for 4−6[a]

	$E_{1/2}$/V	
complex	metal-based oxidations	ligand-based reductions
4	+1.220	−0.475, −0.720, −0.960
5	+1.350	−0.550[b], −0.870[b], −1.140[b], −1.540[b]
6	+1.415	−0.495, −1.015[b], −1.460[b]

[a]Conditions: vs Ag/AgCl, CH_3CN, 0.1 M $[^tNBu_4]PF_6$, under N_2, 25 °C. [b]Reductions are not fully chemically reversible, only $E_{p,c}$ values are quoted.

reversible oxidation assigned to the $Ru^{III/II}$ couple at slightly lower voltage than observed for their dppn analogue; they all also display several reduction processes.

Previous studies have revealed that the free qdppn ligand displays three irreversible reduction peaks at Ep = −0.665, −1.295, and −1.540 V (versus Ag/AgCl in acetonitrile), which were assigned to redox processes located on different fragments of the molecule: semiquinone formation, the reduction of the pyrazine fragment, and then the reduction of the phenanthroline portions of qdppn, respectively.[10] All three of the new complexes display a low lying reduction (<−0.6 V); thus, through comparison with the free ligand we assign this to a qddpn-based quinone/semiquinone reduction, which is anodically shifted because of coordination to the metal cation.

Photophysical Studies. The UV−Visible spectra of the three new complexes recorded in acetonitrile solution, Table 4,

Table 4. Absorption Spectra of Complexes 4−6[a]

	λ/ nm (10^{-3} ε/ M^{-1} cm^{-1})
qddpn	244 (43.7), 277 (34.9), 322 (31.9)
4	243 (40.5), 279 (61.8), 310 (59.5), 351 (29.2), 438 (7.5), 506 (3.1) and 510 (3.6)
5	231sh (33.5), 274 (54.6), 307 (50.0), 349sh (16. 0), 408 (6.9), 475 (4.100)
6	202 (81), 223 (77), 263 (105), 308 (43.7), 439 (18.3).

[a]As hexafluorophosphate salts recorded in acetonitrile at room temperature.

are dominated by high-energy bands between 270−310 nm which correspond to $\pi\rightarrow\pi^*$ transitions within the aromatic nitrogen donor ligands. The UV−Visible spectrum of the qdppn ligand in acetonitrile exhibits three bands at 242, 274,

dx.doi.org/10.1021/ic201914h | Inorg. Chem. 2012, 51, 463−471

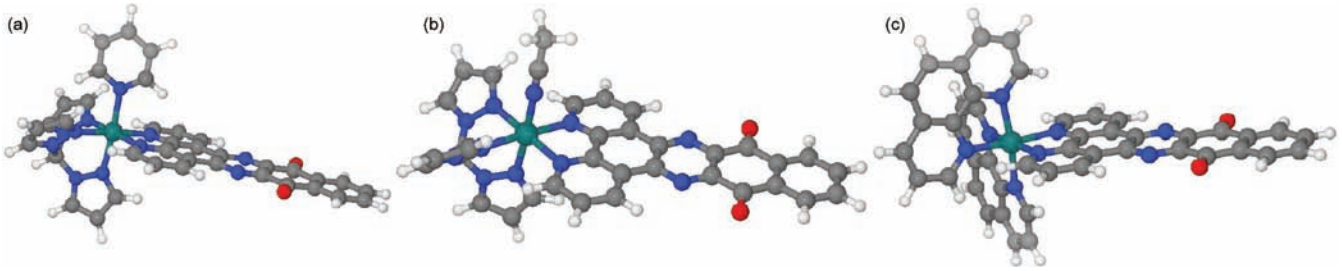

Figure 5. DFT optimized structures of compounds **4**–**6**.

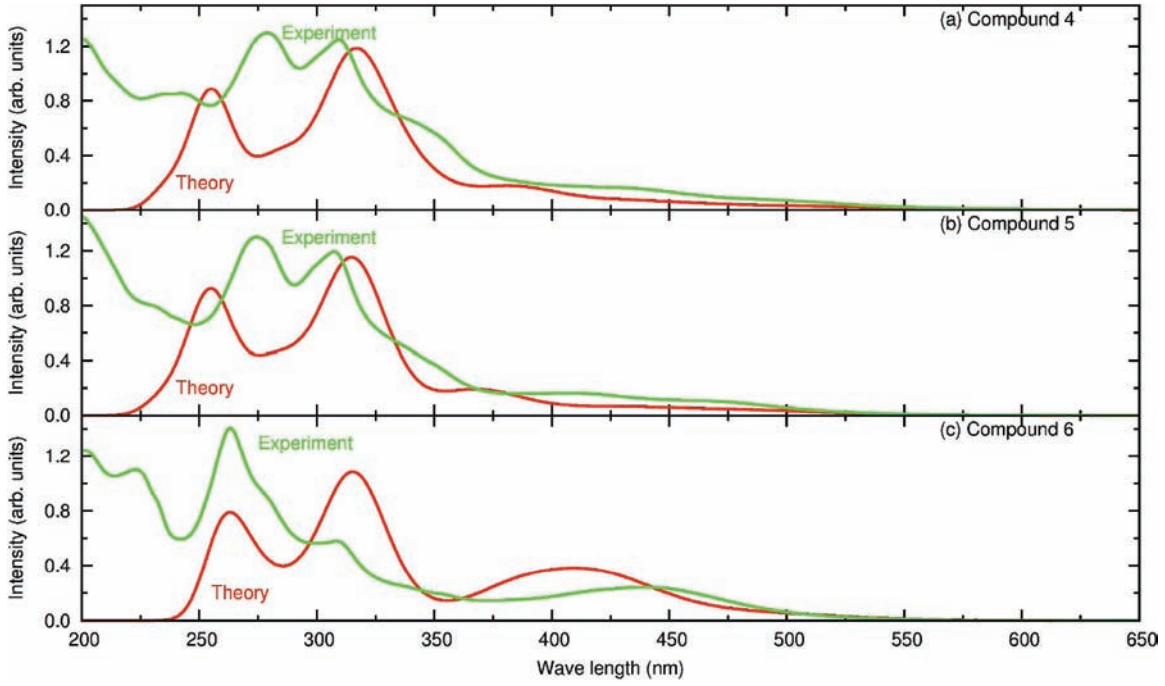

Figure 6. Calculated spectra versus experimental spectra for complexes **4**–**6**.

and 315 nm; the first two bands have previously been assigned to intraligand $\pi\rightarrow\pi^*$(qdppn) transitions and the third to a n→π^*(qdppn) transition.[10] Consequently, the moderately intense bands in the near-UV regions for complexes **4** (243 nm, 279 nm, 310 nm), **5** (274 and 307 nm), and **6** (263 nm, and, 308 nm) are assigned to qdppn-based transitions.

Broad Ru(dπ)→qdppn(π^*) ^{1}MLCT bands are also observed in the visible region of the spectra, appearing in the region of the spectrum typical for ruthenium(II) complexes with coordinated polyimine ligands; however, the maxima for the ^{1}MLCT bands of the qdppn complexes are red-shifted and extend further into the visible region compared to their respective dppn counterparts.

No appreciable luminescence was found for complexes **4**–**6** in MeCN solution. In this case, similar to the data reported for related species containing quinone-based ligands, we suggest that the ^{3}MLCT {Ru-to-dppn} excited state is quenched via electron transfer to the quinone moiety of the ligand.

Given the low-lying qdppn-based unoccupied orbitals in the complexes demonstrated by their reduction potential values (Table 4), nanosecond resolved absorption spectroscopic studies were used to investigate the possible generation of a charge-separated state located on the quinone moiety of the coordinated qdppn. The experiments were performed in acetonitrile and water, using appropriate salts. However, in a 22 ns time scale (and longer) no ground state bleaches or transient signals were observed in the range from 380 to 700 nm. Within the limitation of the equipment used this insinuates an upper limit for any charge separated excited state of around <7 ns, appreciably smaller than the $\pi\rightarrow\pi^*$excited state lifetimes observed in dppn-based analogues, for example, the 62 μs found for **3** in similar conditions.[17] A similar short-lived excited state (<20 ns) was found for the [Re(CO)$_3$Cl(aqphen)] complex,[6a] which was taken to indicate that aqphen could function as an acceptor site in chromophore-quencher assembly, a hypothesis that has subsequently been experimentally proven.[6a] Given its similarities with aqphen, it is clear that qdppn has potential in a similar role.

Singlet Oxygen Sensitization. The efficiency of the [Ru^{II}(dppq)] complexes toward singlet oxygen sensitization was assessed by the direct measurement of ^{1}O$_2$ near-infrared luminescence. Irradiation of aerated solutions of complexes was accompanied by the generation of singlet oxygen, as indicated by the appearance of a characteristic ^{1}O$_2$($^1\Delta_g$) → ^{3}O$_2$ phosphorescence at 1270 nm. The yield of the formation of ^{1}O$_2$, ϕ(^{1}O$_2$), was determined by measuring its phosphorescence intensity using an optically matched solution of phenalenone as a reference sensitizer.

The different excited state character of the qdppn based complexes relative to their dppn analogues is also reflected in

dx.doi.org/10.1021/ic201914h | *Inorg. Chem.* 2012, 51, 463–471

Table 5. Major Absorption Transitions for Complex 6 As Obtained through TD-DFT Calculations

no.	energy (cm^{-1})	wavelength (nm)	osc. strength	major contributions
11	23141	432.13	0.09	H-2→L+2 (71%), H-2→L+3 (24%)
13	23707	421.81	0.11	H-2→L+2 (15%), H-2→L+3 (37%), H-1→L+4 (43%)
14	23973	417.13	0.10	H-2→L+4 (52%), H-1→L+3 (36%)
21	25935	385.58	0.11	H-1→L+4 (10%), H-1→L+5 (21%), HOMO→L+7 (57%)
44	31572	316.74	0.97	H-10→LUMO (25%), H-9→L+1 (27%), H-5→L+1 (44%)
45	32138	311.16	0.08	H-9→L+1 (37%), H-5→L+1 (33%), H-3→L+2 (10%)
53	33430	299.13	0.10	H-12→LUMO (85%)
55	33874	295.21	0.10	H-12→L+1 (69%), H-2→L+8 (12%)
86	37524	266.50	0.08	H-5→L+5 (64%)
90	37904	263.82	0.09	H-7→L+5 (19%), H-5→L+6 (31%), H-1→L+10 (12%)
99	38553	259.38	0.26	H-7→L+4 (10%), H-1→L+11 (34%)
100	38605	259.03	0.14	H-2→L+11 (10%), HOMO→L+12 (29%)

their capabilities as singlet oxygen sensitizers. We have previously shown that photoexcitation of Ru^{II} complexes containing coordinated dppn ligand produce $^1O_2$ with high yield:[17] for example, photoexcitation of **2** produces singlet oxygen with the yield of $\varphi(^1O_2)$ = 75%; yet in the same conditions, **5** yields a value of $\varphi(^1O_2)$ = 2.3%, confirming that Ru(dppq) systems are poor singlet oxygen sensitizers. The phosphorescence lifetime of singlet oxygen produced by the complexes and by the reference sensitizer phenalenone, was the same (~ 80 μs in acetonitrile), confirming that $^1O_2$ does not react with the ground state of the Ru(dppn) complexes.

DFT Studies. We performed calculations on **4**–**6** using the procedure outlined in the Experimental Section. In the case of **4** and **5** we adapted the optimized structures for their dppn equivalents, which we recently reported.[16,17] In the case of **6** we used the crystal structure reported above. In all cases no counterions were included in the calculations. The resultant structures, given in Figure 5, are as expected from the experimental data.

For compound **4** a structure with the pyridine ring at 90 degrees to its current position is also possible; however, as in our previous study on related dppz-based systems,[15d] this geometry is significantly higher in energy than the one depicted in Figure 5. We then calculated the expected absorption spectra associated with these optimized structures. One hundred states were included in our calculations. In our experience this allows a comparison with the experimental spectrum down to approximately 200–210 nm. The calculated spectra are given in Figure 6.

As is clear from these figures, we obtain a reasonable agreement with experiment. It is not entirely clear why the agreement in this case is not as close as that obtained for related systems we have recently reported.[34] Attempts to obtain better agreement using different functionals were unsuccessful. It may be that hydrogen-bonding involving the water molecules causes this discrepancy. Attempts to model this by placing two water molecules around compound **6** had no significant effect. Unfortunately, because of the large number of possible configurations, adding more water molecules requires significantly more computational resources than are currently available to us.

Since comparisons of experimental and theoretical data for each of the three UV–vis spectra are similar, we present a detailed description for complex **6** herein and refer to the Supporting Information for descriptions on the other two; furthermore, a complete list of transitions for each of the complexes with oscillator strengths larger than 0.04 is given in the Supporting Information. Herein, we tabulate the main transitions (f > 0.08) for **6** in Table 5. The most important frontier orbitals for this compound are given in Figure 7. Again a complete set from HOMO-5 to LUMO+5 for each of the compounds is given in the Supporting Information.

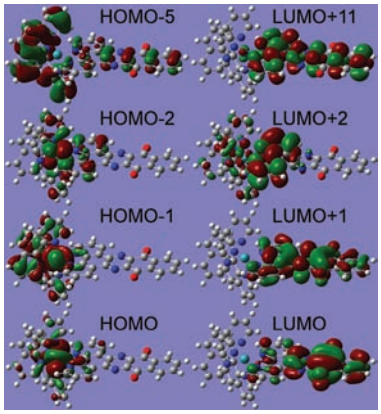

Figure 7. Selected Frontier orbitals for compound **6**.

As is clear from Table 5, the lower energy transitions are dominated by transitions from HOMO-2/HOMO-1 to LUMO +2/LUMO+3/LUMO+4. These transitions can be classified as MLCT transitions from Ru to an orbital on either the phen ligands [LUMO+3/LUMO+4 (see Supporting Information)] or the phen moiety of the qdppn ligand (LUMO+2). The major transition at 316.74 nm and transitions at higher energies are all π–π^* based as is clear from the orbital assignments and Figure 7. The dominant transition for the 316.74 nm peak is in fact a phen→qdppn ligand-to-ligand charge-transfer transition, although intraligand transitions occur as well. In fact such labels are qualitative at best, since most transitions contain contributions from a number of different classes of transitions at the same time.

DNA Binding Studies. Water-soluble chloride salts of **4**, **5**, and **6** were obtained via anion metathesis of their respective PF_6^- salts using [nBu$_4$N]Cl in acetone.

No detectable emission was observed upon addition of CT-DNA to aqueous solutions of the new complexes. Therefore their interaction with CT-DNA in aqueous buffer (25 mM NaCl, 5 mmol tris, pH 7.0) was investigated using UV–visible spectroscopic titrations and compared to the previously reported data for their dppn-based analogues.[16] Although no appreciable bathochromic shifts in the π→π^* bands, such as

dx.doi.org/10.1021/ic201914h | Inorg. Chem. 2012, 51, 463–471

those that occur for $[1]Cl_2$ and $[2]Cl_2$, are observed,[16] addition of small aliquots of CT-DNA to buffer solutions of the complexes result in large hypochromicity in both MLCT and $\pi\rightarrow\pi^*$ absorption bands, see Figure 8. The raw data produced typical saturation binding curves (inset Figure 5).

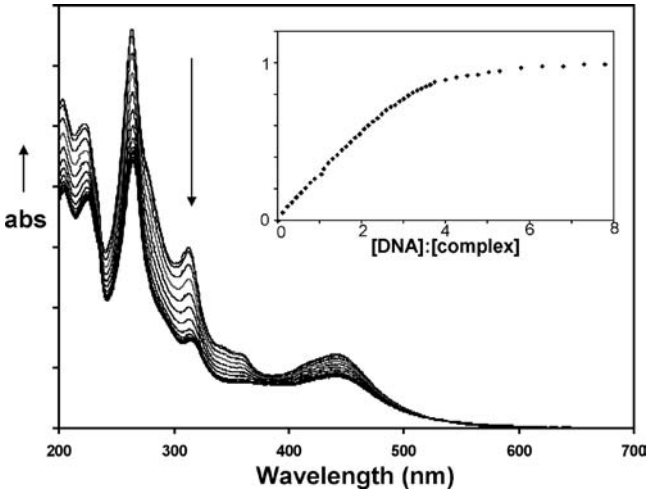

Figure 8. Electronic spectral trace of $[3]Cl_2$ in buffer (25 mM NaCl, 5 mmol tris, pH 7.0) upon addition of double-stranded CT-DNA. Inset, binding curve for $[3]Cl_2$.

Fits of data to the McGhee–Von Hippel (MVH) model[35], Table 6, indicate that **4**–**6** have bonding affinities between 5.7

Table 6. Selected Binding Parameters for the New qdppn-Based Complexes with CT-DNA[a]

complex	K_b ($dm^3\ mol^{-1}$)	S (bp)
4	5.7×10^5	2.1
5	7.2×10^5	1.1
6	8.0×10^5	2.8

[a]Conditions: aqueous buffer (25 mM NaCl, 5 mmol tris, pH 7.0).

$\times 10^5$–$8 \times 10^5\ M^{-1}$. These binding affinities are approximately an order of magnitude lower than those obtained for **1**–**3** and analogous dppz-based complexes. Given that the ancillary ligands for the pairs of complexes **1** and **4**, **2** and **5**, and also **3** and **6** are identical, the differences in binding affinity between these pairs of complexes can only be due to the change of intercalative ligand.

Although these observations are consistent with the interaction of a metallo-intercalator and DNA, definitive proof can be provided by viscosity studies, as intercalation results in a lengthening of DNA thus producing a concomitant increase in the relative specific viscosity of aqueous DNA solutions.[36] We found that the relative specific viscosity of CT-DNA does significantly increase upon addition of Ru(qdppn) complexes, and these changes are comparable with the parent dppn-based systems which are known intercalators; the Supporting Information shows a typical experiment involving $[6]Cl_2$, all the complexes produce similar results.

CONCLUSIONS

Although the DNA binding properties of **4**– **6** are comparable to their dppz and dppn analogues, the properties of their excited states are much more distinctive. In contrast to dppn complexes, which our previous studies have shown are nonemissive because of a low lying dppn-based $\pi\rightarrow\pi^*$ excited state, qdppn complexes are nonluminescent because of the formation of a short-lived charge separated state, where the initial excited state is quenched via electron transfer to the quinone moiety of the ligand.

Previous reports on a related aqphen system have shown that the excited states of quinone-based DNA-intercalating complexes are capable of cleaving DNA and have also shown that reduction of the quinone moiety of the ligand to a hydroquinone moiety results in an emissive system.[7,8] Studies investigating whether qdppn complexes display similar properties are currently underway and will form the basis of future reports.

ASSOCIATED CONTENT

Supporting Information

Cartesian Coordinates, TD-DFT calculations and frontier orbitals for complexes **4**, **5**, and **6**. Relative specific viscosity changes for an aqueous buffered solution of CT-DNA upon addition of $[6]Cl_2$. This material is available free of charge via the Internet at http://pubs.acs.org.

AUTHOR INFORMATION

Corresponding Author

*Fax: +44 (0)114 222 9346. Phone: +44 (0)114 222 9325. E-mail: james.thomas@sheffield.ac.uk (J.A.T.), a.meijer@sheffield.ac.uk (A.J.H.M.M.).

ACKNOWLEDGMENTS

We gratefully acknowledge the support of the BBSRC (S.P.F., M.W., and J.A.T), the EPSRC (advanced fellowship to J.A.W.), and the University of Sheffield, and the White Rose Consortia (S.C.P.). We are grateful to Dr. I. V. Sazanovich, Dr. R. Edge, and Dr. S. Navaratnam for experimental assistance. We are grateful for the diligence of the referees.

REFERENCES

(1) (a) Juris, A.; Balzani, V.; Barigelletti, F.; Campagna, S.; Belser, P.; Von Zelewsky. *Coord. Chem. Rev.* **1988**, *84*, 85. (b) Schanze, K. S.; McQueen, D. B.; Perkins, T. A.; Cabana, L. A. *Coord. Chem. Rev.* **1993**, *122*, 63. (c) Balzani, V.; Juris, A.; Venturi, M.; Campagna, S.; Serroni, S. *Chem. Rev.* **1996**, *96*, 759. (d) Dixon, I. M.; Collin, J.-P.; Sauvage, J.-P.; Flamigni, L.; Encinas, S.; Barigelletti, F. *Chem. Soc. Rev.* **2000**, *29*, 385. (e) Striplin, D. R.; Crosby, G. A. *Coord. Chem. Rev.* **2000**, *211*, 163. (f) Baranoff, E.; Collin, J.-P.; Flamigni, L.; Sauvage, J.-P. *Chem. Soc. Rev.* **2004**, *33*, 147. (g) Hofmeier, H.; Schubert, U. S. *Chem. Soc. Rev.* **2004**, *33*, 373. (h) Huynh, M. H. V.; Dattelbaum, D. M.; Meyer, T. M. *Coord. Chem. Rev.* **2005**, *249*, 457. (i) You, Y.; Park, S. Y. *Dalton. Trans.* **2009**, 1267.

(2) (a) Brunschwig, B. S.; Chou, M. H.; Creutz, C.; Ghosh, P.; Sutin, N. *J. Am. Chem. Soc.* **1983**, *105*, 4832. (b) Hagfeldt, A.; Grätzel, M. *Acc. Chem. Res.* **2000**, *33*, 269. (c) Grätzel, M. *Nature* **2001**, *414*, 338. (d) Serroni, S.; Campagna, S.; Puntoriero, F.; Di Pietro, C.; McClenaghan, N.; Loiseau, F. *Chem. Soc. Rev.* **2001**, *30*, 367. (e) Youngblood, W. J.; Lee, S.-H. A.; Maeda, K.; Mallouk, T. E. *Acc. Chem. Res.* **2009**, *42*, 1966.

(3) (a) Balzani, V.; Juris, A.; Venturi, M.; Flamigni, L.; Campagna, S.; Serroni, S. *Chem. Rev.* **1996**, *96*, 759. (b) Flamigni, L.; Barigelletti, F. *Chem. Soc. Rev.* **2000**, *29*, 1. (c) Balzani, V.; Ceroni, P.; Juris, A.; Venturi, M.; Flamigni, L.; Campagna, S.; Puntoriero, F.; Serroni, S. *Coord. Chem. Rev.* **2001**, *219*, 545. (d) Balzani, V.; Credi, A.; Venturi, M. *Molecular Devices and Machines: A Journey into the Nano World*; Wiley-VCH: Weinheim, Germany, 2003. (e) García-Cañadas, J.; Meacham, A. P.; Peter, L. M.; Ward, M. D. *Angew. Chem., Int. Ed.*

2003, *42*, 3011. (f) Balzani, V.; Clemente-Leon, M.; Credi, A.; Ferrer, B.; Venturi, M.; Flood, A. H.; Stoddart, J. F. *Proc. Natl. Acad. Sci. U.S.A.* **2006**, *103*, 1178. (g) Champin, B.; Mobian, P.; Sauvage, J.-P. *Chem. Soc. Rev.* **2007**, *36*, 358.

(4) (a) *Functions of Quinones in Energy Conserving Systems*; Trumpower, B. I., Ed.; Academic Press: New York, 1986. (b) Wasielewski, M. R. *Chem. Rev.* **1992**, *92*, 435. (c) Kurreck, H.; Huber, M. *Angew. Chem., Int. Ed. Engl.* **1995**, *34*, 849. (d) Ward, M. D. *Chem. Soc. Rev.* **1997**, *26*, 365.

(5) (a) Gebicki, J.; Marcinek, A.; Zielonka, J. *Acc. Chem. Res.* **2004**, *37*, 379. (b) Wu, H.; Zhang, D.; Su, L.; Ohkubo, K.; Zhang, C.; Yin, S.; Mao, L.; Shuai, Z.; Fukuzumi, S.; Zhu, D. *J. Am. Chem. Soc.* **2007**, *129*, 6839. (c) Yuasa, J.; Yamada, S.; Fukuzumi, S. *Angew. Chem., Int. Ed.* **2008**, *47*, 1068.

(6) (a) López, R.; Loeb, B.; Boussie, T.; Meyer, T. J. *Tetrahedron Lett.* **1996**, *37*, 5437. (b) López, R. B.; Leiva, A. M.; Zuloaga, F.; Loeb, B.; Norambuena, E.; Omberg, K. M.; Schoonover, J. R.; Striplin, D.; Devenney, M.; Meyer, T. J. *Inorg. Chem.* **1999**, *38*, 2924.

(7) Arounaguiri, S.; Maiya, B. G. *Inorg. Chem.* **1999**, *38*, 842.

(8) Ambroise, A.; Maiya, B. G. *Inorg. Chem.* **2000**, *39*, 4256.

(9) Dupont, N.; Ran, Y.-F.; Jia, H.-P.; Grilj, J.; Ding, J.; Liu, S.-X.; Deurtins, S.; Hauser, A. *Inorg. Chem.* **2011**, *50*, 3295.

(10) Díaz, R.; Reyes, O.; Francois, A.; Leiva, A. M.; Loeb, B. *Tetrahedron Lett.* **2001**, *42*, 6463.

(11) Rau, S.; Schwalbe, M.; Losse, S.; Görls, H.; McAlister, C.; MacDonnell, F. M.; Vos, J. G. *Eur. J. Inorg. Chem.* **2008**, 1031.

(12) Friedman, A. E.; Chambron, J.-C.; Sauvage, J.-P.; Turro, N. J.; Barton, J. K. *J. Am. Chem. Soc.* **1990**, *112*, 4960.

(13) Erkkila, K. E.; Odom, D. T.; Barton, J. K. *Chem. Rev.* **1999**, *99*, 2777. Zeglis, B. M.; Pierre, V. C.; Barton, J. K. *Chem. Commun.* **2007**, 4565.

(14) Metcalfe, C.; Thomas, J. A. *Chem. Soc. Rev.* **2003**, *32*, 215.

(15) (a) Metcalfe, C.; Adams, H.; Haq, I.; Thomas, J. A. *Chem. Commun.* **2003**, 1152. (b) Metcalfe, C.; Haq, I.; Thomas, J. A. *Inorg. Chem.* **2004**, *43*, 317. (c) Foxon, S. P.; Phillips, T.; Gill, M. R.; Towrie, M.; Parker, A. W.; Webb, M.; Thomas, J. A. *Angew. Chem., Int. Ed.* **2007**, *46*, 3686. (d) Waywell, P.; Gonzalez, V.; Gill, M. R.; Adams, H.; Meijer, A. J. H. M.; Williamson, M. P.; Thomas, J. A. *Chem.—Eur. J.* **2010**, *16*, 2407.

(16) Foxon, S. P.; Metcalfe, C.; Adams, H.; Webb, M.; Thomas, J. A. *Inorg. Chem.* **2007**, *46*, 409.

(17) Foxon, S. P.; Alamiry, M. A. H.; Walker, M. G.; Meijer, A. J. H. M.; Sazanovich, I. V.; Weinstein, J. A.; Thomas, J. A. *J. Phys. Chem. A* **2009**, *113*, 12754.

(18) Hartshorn, R. M.; Barton, J. K. *J. Am. Chem. Soc.* **1992**, *114*, 5919.

(19) Choi, S.-D.; Kim, M.-S.; Kim, S. K.; Lincoln, P.; Tuite, E.; Nordén, B. *Biochemistry* **1997**, *36*, 214.

(20) Sun, Y.; Joyce, L. E.; Dickson, N. M.; Turro, C. *Chem. Commun.* **2010**, *46*, 2426.

(21) Paw, W.; Eisenberg, R. *Inorg. Chem.* **1997**, *36*, 2287.

(22) Sullivan, B. P.; Salmon, D. J.; Meyer, T. J. *Inorg. Chem.* **1978**, *17*, 3334.

(23) Winkelmann, E. *Tetrahedron* **1969**, *25*, 2427.

(24) Frisch, M. J.; Trucks, G. W.; Schlegel, H. B.; Scuseria, G. E.; Robb, M. A.; Cheeseman, J. R.; Scalmani, G.; Barone, V.; Mennucci, B.; Petersson, G. A.; Nakatsuji, H.; Caricato, M.; Li, X.; Hratchian, H. P.; Izmaylov, A. F.; Bloino, J.; Zheng, G.; Sonnenberg, J. L.; Hada, M.; Ehara, M.; Toyota, K.; Fukuda, R.; Hasegawa, J.; Ishida, M.; Nakajima, T.; Honda, Y.; Kitao, O.; Nakai, H.; Vreven, T.; Montgomery, Jr., J. A.; Peralta, J. E.; Ogliaro, F.; Bearpark, M.; Heyd, J. J.; Brothers, E.; Kudin, K. N.; Staroverov, V. N.; Kobayashi, R.; Normand, J.; Raghavachari, K.; Rendell, A.; Burant, J. C.; Iyengar, S. S.; Tomasi, J.; Cossi, M.; Rega, N.; Millam, N. J.; Klene, M.; Knox, J. E.; Cross, J. B.; Bakken, V.; Adamo, C.; Jaramillo, J.; Gomperts, R.; Stratmann, R. E.; Yazyev, O.; Austin, A. J.; Cammi, R.; Pomelli, C.; Ochterski, J. W.; Martin, R. L.; Morokuma, K.; Zakrzewski, V. G.; Voth, G. A.; Salvador, P.; Dannenberg, J. J.; Dapprich, S.; Daniels, A. D.; Farkas, Ö.; Foresman, J. B.; Ortiz, J. V.; Cioslowski, J.; Fox, D. J. *Gaussian 09*, Revision A.1; Gaussian, Inc.: Wallingford, CT, 2009.

(25) Becke, A. D. *J. Chem. Phys.* **1993**, *98*, 5648.

(26) (a) Nicklass, A.; Dolg, M.; Stoll, H.; Preuss, H. *J. Chem. Phys.* **1995**, *102*, 8942. (b) Cao, X. Y.; Dolg, M. *J. Chem. Phys.* **2001**, *115*, 7348 and references therein.

(27) (a) McLean, A. D.; Chandler, G. S. *J. Chem. Phys.* **1980**, *72*, 5639. (b) Krishnan, R.; Binkley, J. S.; Seeger, R.; Pople, J. A. *J. Chem. Phys.* **1980**, *72*, 650.

(28) (a) Menucci, B.; Tomassi, J. *J. Chem. Phys.* **1997**, *106*, 5151–5158. (b) Cossi, M.; Barone, V.; Menucci, B.; Tomassi, J. *Chem. Phys. Lett.* **1998**, *286*, 253–260, and references therein.

(29) (a) Strattmann, R. E.; Scuseria, G. E.; Frisch, M. J. *J. Phys. Chem.* **1998**, *108*, 4439. (b) Bauernschmidt, R.; Ahlrichs, R. *Chem. Phys. Lett.* **1996**, *256*, 454. (c) Casida, M. E.; Jamorski, C.; Casida, K. C.; Salahub, D. R. *J. Chem. Phys.* **1998**, *108*, 4439.

(30) O'Boyle, N. M.; Tenderholt, A. L.; Langner, K. M. *J. Comput. Chem.* **2008**, *29*, 839.

(31) Sheldrick, G. M. *SHELXS-97, A Program for Automatic Solution of Crystal Structures*; University of Göttingen: Göttingen, Germany, 1997.

(32) Sheldrick, G. M. *SHELXL-97, A Program for Crystal Structure Refinement*; University of Göttingen: Göttingen, Germany, 1997.

(33) Kim, M.-J.; Konduri, R.; Ye, H.; MacDonnell, F. M.; Puntoriero, F.; Serroni, S.; Campagna, S.; Holder, T.; Kinsel, G.; Rajeshwar, K. *Inorg. Chem.* **2002**, *41*, 2471.

(34) Ahmad, H.; Meijer, A. J. H. M.; Thomas, J. A. *Chem.—Asian J.* **2011**, *6*, 2339.

(35) McGhee, J. D.; von Hippel, P. H. *J. Mol. Biol.* **1974**, *86*, 469.

(36) Satyanarayana, S.; Dabrowiak, J. C.; Chaires, J. B. *Biochemistry* **1992**, *31*, 9319.